Thrust allocation with dynamic power consumption modulation for diesel-electric ships

Aleksander Veksler, *Member, IEEE,* Tor Arne Johansen, *Senior Member, IEEE,*
Roger Skjetne, *Member, IEEE,* and Eirik Mathiesen, *Member, IEEE.*

***Abstract*—Modern ships and offshore units built for dynamic positioning are often powered by an electric power plant consisting of two or more diesel-electric generators. Actuation in any desired direction is achieved by placing electrical thrusters at suitable points on the hull. Such ships usually also have other large electrical loads. Operations in the naturally unpredictable marine environment often necessitate large variations in power consumption, both by the thrusters and by the other consumers. This wears down the power plant, and increases the fuel consumption and pollution. This paper introduces a thrust allocation algorithm that facilitates more stable loading on the power plant. This algorithm modulates the power consumption by coordinating the thrusters to introduce load variations that counteract the load variations from the other consumers on the ship. To reduce load variations without increasing overall power consumption it is necessary to deviate from the thrust command given by the dynamic positioning system. The resulting deviations in position and velocity of the vessel are tightly controlled, and the results show that small deviations are sufficient to fulfill the objective of reducing the load variations. The effectiveness of the proposed algorithm has been demonstrated on a simulated vessel with a diesel-electric power plant. A model for simulation of a marine power plant for control design purposes has been developed.**

***Index Terms*—marine vehicles, dynamic positioning, power system control, thrust allocation, load management, distributed power generation, marine power plant, electric propulsion.**

I. Introduction

A marine vessel is said to have dynamic positioning (DP) capability if it is able to maintain a predetermined position and heading automatically exclusively by means of thruster force [1]. DP is therefore an alternative, and sometimes a supplement to the more traditional solution of anchoring a ship to the seabed. The advantages of positioning a ship with the thrusters instead of anchoring it include:

- Immediate position acquiring and re-acquiring. A position setpoint change can usually be performed by a command from the operator station, whereas a significant position setpoint change for an anchored vessel would require repositioning the anchors.
- Ability to operate on unlimited depths. While anchors can operate on depths of only up to about 500 meters, no such limitations exist with dynamic positioning.
- No risk of damage to seabed infrastructure and risers, which allows safe and flexible operation in crowded offshore production fields.
- Accurate control of position and heading.

The main disadvantages are that a ship has to be specifically equipped to operate in DP, and that dynamically positioned ships often need to spend large amounts of energy to stay in position.

DP is usually installed on offshore service vessels, on drill rigs, and now increasingly on production platforms that are intended to operate on very deep locations.

To maximize the capability of the DP system, the thrusters should be placed on distant locations on the ship, which makes mechanical transfer of power from the engines less practical compared to electrical distribution. This and other operational advantages [2, p. 6] result in electric power distribution being almost ubiquitous in offshore vessels with DP today.

The type of prime mover predominantly in use is the diesel engine, although other types such as gas engines and gas turbines are also available. A power grid on a DP vessel typically consists of several diesel generators connected to the thrusters and other consumers through a reconfigurable distribution network with several separable segments and several voltage levels. Often, the thruster system requires more power from the generators than all the other consumers on the grid combined. The control architecture for the resulting system is highly distributed, with independent controllers for diesel engine fuel injection, generator rotor magnetization, circuit breakers, centralized and local thruster controllers, etc. An example of such network with controllers is shown on Figure 1. In legacy implementations in the literature and the industry, many of the controllers do not directly communicate with each other, but instead gain information about the state of the grid by monitoring voltage levels, currents and the frequency on the bus. This has changed in the recent years with increased communication between the individual controllers through data networks.

While diesel engines are efficient in terms of fuel consumption [3], use of primarily diesel electric power grid introduces a range of challenges for the control system in terms of both stability and fuel efficiency. Stability relates to maintaining stable frequency and voltage on the grid in presence of large and sometimes unpredictable disturbances in load, as well as stable load sharing when a grid segment is powered by

Aleksander Veksler and Tor Arne Johansen are with the center for Autonomous Marine Operations and Systems, Department of Engineering Cybernetics (NTNU), Norway. (e-mail: aleksander.veksler@itk.ntnu.no, tor.arne.johansen@itk.ntnu.no)

Roger Skjetne is with the Department of Marine Technology, Norwegian University of Science and Technology (NTNU), Norway. (e -mail: roger.skjetne@ntnu.org)

Eirik Mathiesen is a principal engineer with Kongsberg Maritime. (e-mail: eirik.mathiesen@kongsberg.com)

Submitted for review

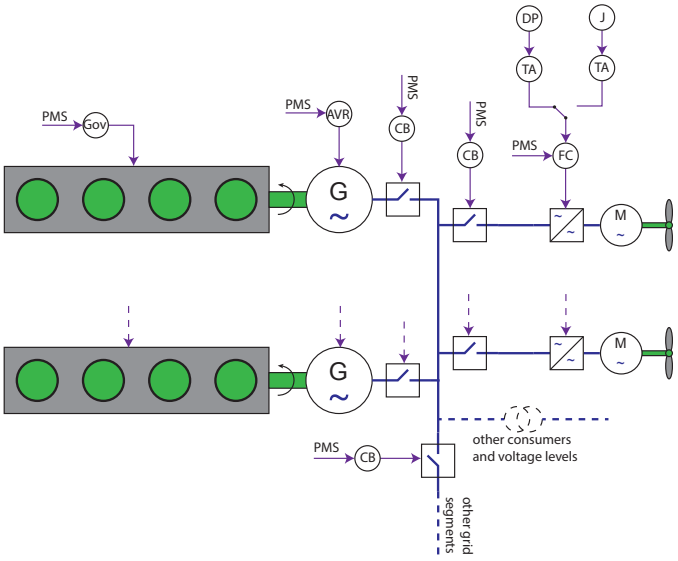

Fig. 1: An illustration showing some of the controllers on the electric grid. A diesel engine speed controller, conventionally called governor (Gov), adjusts the amount of fuel injected into the engines; An Automatic Voltage Regulator (AVR) adjusts the magnetization of the rotor coils of the generators (G); various circuit breakers (CB) connect and disconnect equipment and also isolate faults such as short circuits; the Frequency Converters (FC) are used for local control of the thruster motors (M), and receive commands from both the Thrust Allocation (TA) and the Power Management System (PMS). Finally, the TA can receive the generalized force command from either the DP control system or from a Joystick (J).

more than one generator set. Modern marine diesel engines are almost always turbocharged. Turbocharging limits how fast the engine can increase its output because increasing the output requires building up pressure in the scavenging receiver, which puts a physical limit on how fast a diesel-electric power plant can increase its output. A rapid load increase can therefore lead to a mismatch between the generated mechanical and consumed electrical power. This mismatch can become unrecoverable even if the load rate constraints on the governors are disabled. The result of this mismatch is deficit consumption that extracts energy from the rotating masses in the engines and the generators. If unchecked, it will lead to a rapid drop in frequency, and then a blackout due to engine stall or protection relay disconnect.

The task of designing an optimal control strategy is made easier beacause the factors that lead to pollution often also lead to increased economic costs, meaning that the economic and environmental concerns are often in agreement. Increased fuel consumption leads to both increased fuel expenses and, under most circumstances, more pollution. Pollutants such as carbon monoxide, unburned hydrocarbons, soot and NO_X emissions constitute a minor part of the combustion process in terms of energy, and have therefore a negligible impact on the engine process [4, p. 194]. However, those emissions tend to increase during load transients, especially upwards transients [5, ch. 5 and p. 37]. Those transients also increase wear-and-tear on the engines because of the resulting thermic expansion and contraction. In addition, load variations on the power plant as a whole may lead to excessive start and stop of generator sets, with additional pollution and wear-and-tear due to cold start transients.

Because of this, variations in the power consumption have recently received increased attention in the literature. A cost term for variations in force produced by the individual thrusters is included in [6], which has a dampening effect on the combined load variations. An approach to handling the power limitations in the optimization process is introduced in [7], together with other power-related features.

Typical thrust allocation algorithms such as [6] and [8] do their best to produce the commanded generalized force at all times, most often by passing this command as a constraint to a numerical optimization solver. However, it can be shown that the high inertia of a ship makes it possible to deviate from this command over short periods of time without affecting the position and velocity of the ship significantly [9]. This makes it possible to exploit the thrusters to improve the load dynamics on the power grid. In terms of energy preservation, the short-term transfer of energy from the thrusters can be thought of as coming from the potential energy stored in the mass of the hull in the field of the environmental forces. The amount of energy that can be made available is thus proportional to the mass of the vessel and the square of the permissible velocity deviation. The distance the ship is allowed to deviate from the setpoint determines the length of time until the thrusters will need to use energy to stop the ship and then turn it around. Several approaches to exploiting this energy has been attempted in the literature. In [10], the local thruster controllers were modified to counteract the variations in frequency on the grid by deviating from the orders they receive from the thrust allocation algorithm. Approaching this task on the local thruster controller level precludes the possibility of estimating and limiting the resulting deviations in the position of the ship, since the individual thruster controllers do not have the information about the actions that the other local controllers are undertaking and cannot compute the deviation in the resultant generalized force. Because of this limitation, in the present work the power redistributing functionality is moved to the thrust allocation algorithm. This is in partial contrast with [11], where the reduction in the thruster load was performed by the PMS, by the way of modifying the "power available" signal to the thruster controllers.

In order to produce the counteracting load variations, the thrusters have to be able to both increase and decrease their power consumption at will. Increasing the power consumption can be achieved by biasing the thrusters as described in Subsection IV-D, simply wasting the superfluous energy. Reducing the power consumption is more complicated. For any feasible thrust command given to the thrust allocation algorithm there exists a minimal value for the power consumption used to create that thrust. The existing thrust allocation algorithms usually attempt to minimize the power consumption, and in practice the power consumption is very close to the minimum. This presents two options to control variations in power con-

sumption. The first option is to maintain a thruster bias reserve for this purpose. When a reduction in power consumption is requested to compensate for an increase elsewhere, the thrust allocation algorithm can release some or all of this bias. Doing this inevitably increases the overall power consumption. The second option is to let the power consumption go below the minimal value needed to execute the thrust command, allowing a temporary deviation between commanded and generated thrust. The thrust allocation algorithm presented here explores the second option. It estimates the resulting error introduced in velocity and position of the vessel, and constrains this error to stay within acceptable parameters.

This paper also introduces a practical and generic model for the turbocharger lag modeling, which is used for power plant simulation. In order to focus on the power management aspects of the method, the study has been limited to thrusters with fixed direction. Several methods for handling variable-direction thrusters have been described in the literature, see e.g. [12].

The present work combines and expands the contributions in [13], [14]. It describes and tests a thrust allocation algorithm that coordinates the thrusters to introduce load variations that counteract load variations from the other consumers on the ship, thus reducing the total load variations on the power plant. The structure of the article is as following: first, the architecture of the relevant control systems on a dynamically-positioned ship is presented in Section II; a mathematical model that describes the motion of a ship at the low velocities that are characteristic of the dynamic positioning applications is developed in Section III; this model is used to formulate an estimate of how much deviations in the thrust allocation affect the velocity and position of the vessel in Subsection III-B; the thrust allocation algorithm is described in Section IV and a simulation study is presented in Section V. The simulation study includes a description of the simulated vessel Subsections V-A–V-F. The specifics of the diesel engine model given in Appendix A.

To keep the presentation concise, following notation is used: For $x \in R^N$, $Q = Q^T \in R^{N\times N} \succ 0$, $Q = LL^T$

$$|x|^p \triangleq [|x_1|^p, |x_2|^p, \dots |x_N|^p]^T \tag{1}$$

$$|x|^p \, sign(f) \triangleq \begin{bmatrix} |x_1|^p \, sign(f_1) \\ |x_2|^p \, sign(f_2) \\ \vdots \\ |x_N|^p \, sign(f_N) \end{bmatrix} \tag{2}$$

Notice that $|x|^p \in \mathbb{R}^N$, and is not a vector norm. Also,

$$\|x\|_Q^2 \triangleq x^T Q x = \|Lx\|_2^2 \tag{3}$$

$\mathcal{L}$ is the one-sided Laplace transform operator.

II. Control system architecture

This section describes the control architecture of a typical DP vessel, and places the presented thrust allocation algorithm within this framework.

Figure 2 shows how the proposed thrust allocation algorithm (highlighted in blue) fits within the overall control strategy of the DP and the power plant. A high level motion control algorithm receives the ship position and velocity reference from e.g. GPS, and generates the force and moment of force (collectively generalized force) reference τ_d that can bring the vessel to the setpoint location. The thrust allocation algorithm attempts to coordinate the thrusters so that the resultant generalized force τ they generate matches that reference.

Most thrust allocation algorithms in the literature follow that reference strictly, however the proposed thrust allocation algorithm introduces small deviations from the reference to improve the conditions for the power plant. Sometimes it reduces the power consumption below the minimal consumption needed to follow the reference (P_{min}), resulting in a temporary deviation in the position of the vessel.

The power management system normally has to approve large variations of load from the largest consumers, and in the proposed implementation it informs the thrust allocation algorithm about imminent variations in the load P_{ff} from other consumers, which, from the point of view of the thrust allocation algorithm, is a feedforward signal. The power management system also informs the thrust allocation algorithm about the maximum available power P_{max}, and the current power consumption P_{prev}.

The local thruster controllers should map the thruster force command f to an RPM command to the local thruster power supply, typically frequency converters. This mapping is non-trivial. For example, [15] proposes a feedback-based strategy that ensures the propeller torque can be set as needed, and in [16] the thruster-hull interactions are modeled, which could make it possible to create local thruster controllers that could compensate for those effects automatically.

III. Consequence analysis of a deviation from the commanded generalized force

In this section, a mathematical model of low-speed movement of a surface vessel is presented. This presentation can be seen as a summary of the more thorough discussions about marine vessel modeling that are available in the literature, such as [17]–[20].

The model is then used to estimate the results of a deviation from the command in the thrust allocation algorithm.

A. Mathematical model

For the purposes of dynamic positioning, a ship is usually modeled as a rigid body in three degrees of freedom: Surge (forward), Sway (sideways) and Yaw (turn around the vertical axis). The model is separated into kinematic and dynamic equations.

1) Kinematics: The position of the ship is described in a locally-flat Cartesian coordinate system, with the origin near the DP setpoint, x-axis pointing towards the North and y-axis pointing towards the East. The orientation of the ship is described as a clockwise rotation with the bow pointing towards the North as the reference. This system of coordinates

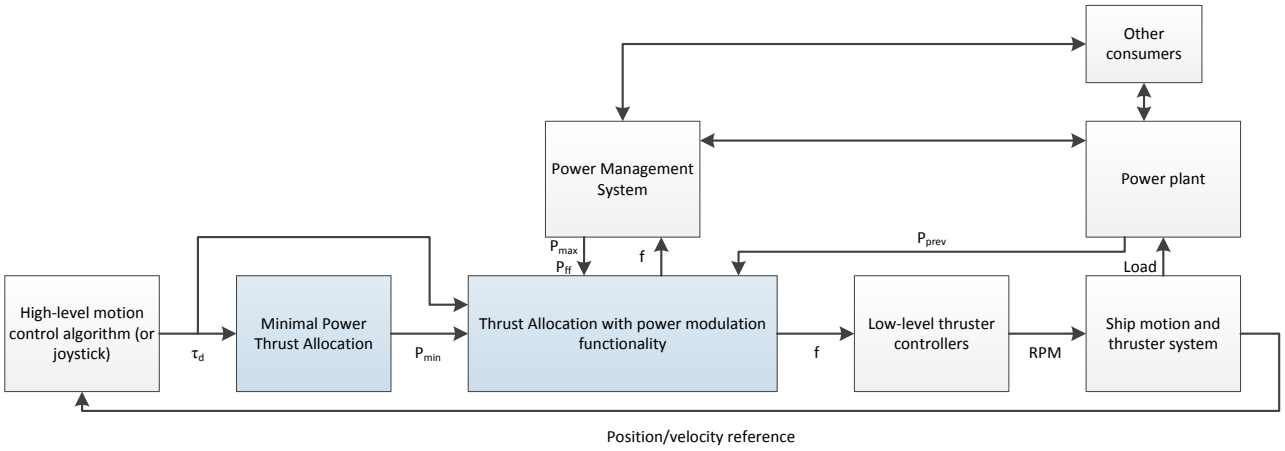

Fig. 2: A general overview of the control architecture.

Symbol	*Description*
$\eta = \begin{bmatrix} N & E & \psi \end{bmatrix}^T \in \mathbb{R}^3$	Position and orientation of the vessel in an inertial frame of reference, in this case North-East-Down.
$\nu = \begin{bmatrix} u & v & r \end{bmatrix}^T \in \mathbb{R}^3$	Velocity of the vessel in its own (body) frame of reference.

TABLE I: Abbreviations that are used to describe the position and velocity of the vessel, as per convention from [21] and [17, especially p. 19].

is called NED. The last letter is an abbreviation for the Down direction.

The velocity of the ship is described in the hull-bound frame of reference, called "body", with the velocity vector composed of forward velocity, lateral velocity and clockwise rotation. This nomenclature was formalized in [21]. A summary of the relevant terms and the conventional abbreviations is presented in Table I.

The relationship between the position in the NED coordinate system and the velocity in the body coordinate system can be represented as

$$\dot{\eta} = R(\psi)\nu \tag{4}$$

where

$$R(\psi) = \begin{bmatrix} \cos(\psi) & -\sin(\psi) & 0 \\ \sin(\psi) & \cos(\psi) & 0 \\ 0 & 0 & 1 \end{bmatrix} \tag{5}$$

2) Dynamics: It is usually most convenient to express the forces that are acting on the ship in the "body" coordinate system.

$$M\dot{\nu} + C(\nu)\nu = \tau_{tot^*} \tag{6}$$

where M is the mass matrix including the hydrodynamic added mass, and τ_{tot^*} is the total resultant generalized force that is acting on the vessel. The centripetal and coriolis term $C(\nu)\nu$ is defined in e.g. [17] or (expanded in the scalar form) in [21].

For low-speed applications the hydrodynamic damping (water resistance) force can be approximated as proportional to the ship velocity, that is $-D\nu$ with D being a constant matrix. The negative sign is purely conventional. The coriolis and centripetal forces may also be ignored. This allows representing (6) as

$$M\dot{\nu} + D\nu = \tau_{tot} \tag{7}$$

where $\tau_{tot} = \tau_{tot^*} + D\nu$.

3) Thruster forces: Let a thruster i located on the ship at the point $\begin{bmatrix} l_{xi} & l_{yi} \end{bmatrix}^T$ and at orientation α_i produce a force equal $K_{ii}f_i$, where $f_i \in \begin{bmatrix} -1 & 1 \end{bmatrix}$. Then, the force this thruster exerts on the ship may be represented as $K_{ii}f_i \begin{bmatrix} \cos\alpha_i & \sin\alpha_i \end{bmatrix}^T$. The torque around the origin of the coordinate system will be $K_{ii}f_i\left(-l_{yi}\cos\alpha_i + l_{xi}\sin\alpha_i\right)$. Collecting the terms above yields

$$\tau_i = K_{ii}f_i \begin{bmatrix} \cos\alpha_i \\ \sin\alpha_i \\ -l_{yi}\cos\alpha_i + l_{xi}\sin\alpha_i \end{bmatrix} \tag{8}$$

Summing up the generalized force from all active thrusters yields the expression for the resultant generalized force from the thrusters,

$$\tau = B(\alpha)Kf \tag{9}$$

where the columns of the matrix $B(\alpha) \in \mathbb{R}^{3\times N}$ consist of $\begin{bmatrix} \cos\alpha_i, & \sin\alpha_i, & \left(-l_{yi}\cos\alpha_i + l_{xi}\sin\alpha_i\right) \end{bmatrix}^{\mathbf{T}}$, and also $f = \begin{bmatrix} f_1 & f_2 & \dots & f_N \end{bmatrix}^T$, $K = \text{diag}\left(K_1, K_2, \dots, K_N\right)$.. This expression is fairly standard in the dynamic positioning literature.

B. Consequences of a force deviation

In this subsection, an approximate expression for the consequences of a small deviation τ_e in the resultant generalized

Fig. 3: The timescape of the real-time implementation. The thrust allocation algorithm is solved iteratively. The output signal is sent to the local thruster controllers at time T, and stays constant until time T_e when the output from the next iteration of the thrust allocation algorithm is available.

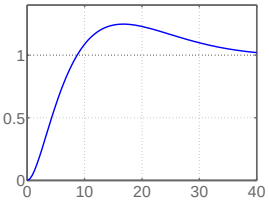

(a) The step response for a surge excitation the high-level motion control algorithm (closed loop) from the simulation in Section V-G.

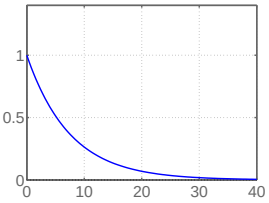

(b) Step response of the high-pass filter, with T_{dp}=8.5 seconds

Fig. 4

thruster force from the command τ_d to the thrust allocation algorithm is formulated.

If τ_e is small enough that the differences in the hydrodynamic forces can be ignored, the deviation in acceleration $\dot{\nu}_e$ can be extracted from (7):

$$\dot{\nu}_e = M^{-1}\tau_e \tag{10}$$

A solution of the thrust allocation algorithm is applied on the vessel for a time period δt, until a new solution is calculated. In typical industrial implementations the thrust allocation problem is solved every second, i.e. $\delta t = 1\,\text{sec}$. Defining T as the time when the current iteration of the thrust allocation algorithm is solved and the output is sent to the thruster controllers, let $T_e = T + \delta t$ be the time when the output from the next iteration of the thrust allocation algorithm is available to the thruster controllers.

If T_e is small enough to assume constant orientation of the ship from 0 to T_e, the deviation in velocity at time T_e can be approximated per

$$\nu_e = \int_0^{T_e} M^{-1}\tau_e dt \tag{11}$$

Under the same assumptions, the deviation in position η_e can be estimated per

$$\eta_e = R\left(\psi_T\right)\int_0^{T_e} \nu_e dt \tag{12}$$

where ψ_T is the orientation of the vessel at time T. The high-level motion control algorithm will also detect the deviations ν_e and η_e introduced by the proposed modifications in the thrust allocation algorithm, and will work to correct them. It will do so on a slower time scale than the thrust allocation algorithm. The thrust allocation algorithm should not correct for the deviations that are already corrected by the high-level motion control algorithm. To estimate how much the position and velocity of the ship deviate from what they would have been had the thrust allocation algorithm followed its command exactly, deviation that is already corrected by the high-level motion control algorithm has to be discarded. One way is to set a specific "hard" time window starting at T_s, and assume that any deviation that was created before that time is corrected by the high-level motion control algorithm by time T

$$\nu_{e,\,h} = M^{-1}\int_{T_s}^{T_e} B(\alpha)Kf(t) - \tau_d(t)dt \tag{13}$$

$$\eta_{e,\,h} = R\left(\psi_T\right)\int_{T_s}^{T_e} \nu_e dt \tag{14}$$

where T_s is a point in time before which it can be assumed that the dynamic positioning algorithm will correct any error. This timeline is illustrated in Figure 3. Stating (14) with a constant rotation matrix $R(\psi)$ is justified as long as $T_e - T_s$ is small enough to assume constant orientation of the ship from T_s to T_e. This approximation was used in [14]. Alternatively, the separation can be done with a soft temporal separation between the TA and the high-level motion control algorithms by using a high-pass filter on the deviation terms. The estimates thus produced will hereby be called ν_e and η_e, with

$$\nu_e(s) = \left[\frac{T_{dp}s}{T_{dp}s+1}\right]\mathcal{L}\left[M^{-1}\int_0^{T_e} B(\alpha)Kf(t) - \tau_d dt\right](s) \tag{15}$$

$$\eta_e(s) = \left[\frac{T_{dp}s}{T_{dp}s+1}\right]\mathcal{L}\left[R\left(\psi_T\right)\int_0^{Te} \nu_e dt\right](s), \tag{16}$$

where T_{dp} is a time constant which represents the bandwidth on which the high-level motion control algorithm operates. Again, the rotation matrix $R(\psi)$ can reasonably be assumed to be constant in (16) as long as the high-pass filter time constant T_{dp} is small enough to mostly filter out the parts of the signal that are old enough for the ship to turn enough to affect the kinematics. Observing that both $\nu_T \triangleq \nu(T)$ and $\eta_T \triangleq \eta(T)$ are known and determined at the current time T, and that $f(t)$ and thus also the inner part of the integral (15) are constant from current time T until the time $T_e = T + \delta t$ when the solution from the next iteration of the thrust allocation algorithm becomes available, the integrals can be separated into past and future terms. High-pass filtering of the future signal can be reasonably discarded since $T_{dp} \gg \delta t$, resulting in the following estimates for the velocity and position deviation due to TA deviating from the command it receives:

$$\hat{\nu}_{e,\,T_e}(s) = \left[\frac{T_{dp}}{T_{dp}s+1}\right]\mathcal{L}\left[M^{-1}\left(B(\alpha)Kf(t) - \tau_d\right)\right](s) + \frac{1}{s}\left(M^{-1}B(\alpha)Kf(T) - \tau_d\right)\delta t \tag{17}$$

$$\hat{\eta}_{e,\,T_e}(s) = \left[\frac{T_{dp}}{T_{dp}s+1}\right] R(\psi_T)\left(\mathcal{L}[\nu_e](s) + \frac{1}{s}\nu_{e,\,T}\delta t\right) + R(\psi_T)\frac{1}{s}\left(M^{-1}\left(B(\alpha)Kf(T)-\tau_d\right)\right)(\delta t)^2/2 \tag{18}$$

The filtering should be performed on the part of the signal starting far enough in the past, until the current time T.

IV. Thrust allocation with power modulation

In this section, a thrust allocation algorithm with a functionality to assist the power management system is described. The numerical optimization problem that is at the core of the method is introduced in Subsection IV-A. Certain implementational aspects are discussed in later subsections.

A. Numerical optimization problem

This subsection presents a mathematical description of the proposed method, with some implementational details left for later. The variables that are used for the thrust allocation algorithms are described in Table II.

1) Minimal power thrust allocation: As the first step, the thrust allocation problem is solved for minimal power consumption without regard to variation in the power consumption:

$$P_{min} = \min_{f,s} P_c K |f|^{3/2} + \|s_0\|^2_{Q_1} \tag{19}$$

subject to

$$B(\alpha)Kf = \tau_d + s_0 \tag{20}$$

$$\underline{f} \le f \le \overline{f} \tag{21}$$

where the power consumption in thrusters is estimated by the nonlinear relationship

$$P_{th} = P_c K |f|^{3/2} \tag{22}$$

which is similar to what was used in [8]. This thrust allocation method is well-documented in the literature, usually with a quadratic power cost function; see [18]. Ideally, the solution of (19)–(21) should fulfill the thrust command τ_d exactly, which would imply that the slack variables satisfy $s_0 \equiv 0$. This may not be possible without violating the constraint (21). Therefore, s must be allowed to be non-zero, with the cost matrix Q_1 being large enough to ensure that s_0 is significantly larger than zero only when constraints (20), (21) would otherwise be infeasible. The constraint (20) therefore ensures that the produced generalized force τ is for practical purposes equal to the commanded force τ_d unless the commanded force is infeasible, while (21) ensures that the thrusters are not commanded to produce more thrust than their maximal capacity. The solution to this optimization problem provides a minimum P_{min} to which the power consumption can be reduced while delivering the requested thrust τ_d, at least as long as the condition $s_0 \approx 0$ holds. This minimum value is used in the following to calculate a control allocation with a specified power bias, P_{bias}, and a feedforward P_{ff} to compensate for power variations in other consumers. The choice of these inputs will be described shortly.

Symbol	*Description*
T	Current time, i.e. time when the thrust allocation problem is solved.
T_e	Time when the solution from the next iteration of the thrust allocation algorithm will be applied to the thrusters.
$\nu_e(t)$, $\eta_e(t)$, $\nu_{e,\,T}$, $\eta_{e,\,T}$	Deviation in, respectively, velocity and position of the vessel from the nominal trajectories, i.e. from what the velocity and position would have been if thrust command was allocated exactly. $\nu_{err}(t)$, $\eta_{err}(t) \in \mathbb{R}^3$ contain longitudinal, lateral, and heading components; $\nu_{e,\,T} \triangleq \nu_e(t=T)$, $\eta_{e,\,T} \triangleq \eta_e(t=T)$.
$\nu_{e,\,max}$, $\eta_{e,\,max}$	Maximal allowed values for $\nu_e(t)$ and $\eta_e(t)$.
τ, τ_d	Actual and desired generalized force produced by all thrusters. τ, $\tau_d \in \mathbb{R}^3$ contain surge and sway forces, and yaw moment.
N	Number of thrusters installed on the ship.
f	$f \in \mathbb{R}^N$, the force produced by individual thrusters. The elements of f are normalized by their maximal values into the range $[-1, 1]$.
K	$K \in \mathbb{R}^{N\times N}$ such that Kf is the vector of forces in Newtons.
$B(\alpha)$	Thruster configuration matrix [18]. It is a function of the vector α consisting of orientations of the individual thrusters. In this paper, α is assumed to be constant.
P_c	$P_c \in \mathbb{R}^{1\times N}$ such that (22) holds.
P_{th}	The total power consumed by the thrusters per (22)
$\dot{P}_{ff}$	The desired rate of change of power consumption by the thrusters. This signal can be used to reduce either frequency or load variations on the electrical network.
P_{min}	Minimal power consumption by the thrusters needed to produce commanded thrust.
P_{max}	The maximal power available for thrust allocation.
ω_g, ω_{0g}	Respectively actual and desired angular frequency of the voltage on the electrical network. Typically, $\omega_{0g} = 2\pi \cdot 60$.
Ψ	$\Psi \succ 0$, quadratic cost matrix of variation in force produced by individual thrusters.
Θ	$\Theta \in \mathbb{R}^+$ is the cost of variation in total power consumption.

TABLE II: Variables used in the thrust allocation model

2) Power modulation functionality: The following optimization problem is used to solve for the actual thrust output:

$$\min_{f,s_1,s_2,\tau_e} P_c K |f|^{3/2} + \left\|K\dot{f}\right\|^2_{\Psi} + \Theta\left(\dot{P}_{th} - \dot{P}_{ff}\right)^2 + \|\tau_e\|^2_{Q_2} + \|s_1\|^2_{Q_3} + \|s_2\|^2_{Q_4} \tag{23}$$

subject to

$$-\nu_{e,\,max} \le \nu_e + s_1 \le \nu_{e,\,max} \tag{24}$$

$$-\eta_{e,\,max} \le \eta_e + s_2 \le \eta_{e,\,max} \tag{25}$$

$$B(\alpha)Kf = \tau_d + \tau_e \tag{26}$$

$$P_{max} \ge P_c K |f|^{3/2} \ge P_{min} + P_{bias} \tag{27}$$

$$\underline{f} \le f \le \overline{f} \tag{28}$$

As a matter of convenience, Table III classifies the variables that are used in the two optimization problems above into

Decision variables	Slack variables	Controllable variables	Physical parameters	Tuning parameters
f	s, τ_e	τ_d, P_{bias}, $\dot{P}_{ff}$, α	P_c, K, $\underline{f}$, $\overline{f}$, P_{max}	Θ, Q_2, Q_3, Q_4, $\nu_{e,max}$, $\eta_{e,max}$

TABLE III: Breakdown of the variables in optimization problems (19)–(21) and (23)–(28)

decision variables, slack variables, controllable variables, *et cetera*. The main decision variable from that controller is the vector f. The problem formulation is instantaneous in the sense that the decision variables (or their derivatives) can only be set once. More precise control could possibly have been achieved allowing the controller to consider the future trajectories for the controlled variables more freely; this would result in an MPC-like formulation. The benefits of such formulation would have to be considered against a large increase in the computational and conceptual complexity. The problem is formulated in continuous time to allow the practitioners the liberty in choosing the discretization method. Simulaiton testing of the algorithm (ref Section V) was however performed exclusively with Forward Euler discretization.

The generalized force order from DP or joystick is represented as τ_d. Contrary to the situation in (19)–(21), significant deviations are expected between the setpoint generalized force τ_d and the actual generalized force $B(\alpha)Kf$. This means that the slack variable in the generalized force constraint (s_0 in (20)) is not longer expected to be close to zero. To emphasize this, it was replaced with τ_e in (26), and weight matrix Q_1 was replaced with Q_2, which should normally have smaller numerical values.

If the operational situation requires a power bias, the constraint (27) ensures that the power consumption in the thrust allocation can be reduced by a selectable parameter P_{bias} while still allocating the commanded thrust. This constraint is only necessary if the bias is required; if it is not it can safely be left out.

If $P_{bias} > P_{max} - P_{min}$, the optimization problem becomes infeasible. Preferably this should be avoided by having enough power available (P_{max}) both to allocate the commanded thrust and to create the required bias, but as a fail-safe the bias could be forced to $P_{bias}^{'} = min(P_{bias}, P_{max} - P_{min})$. A situation with a negative value of $P_{bias}^{'}$ is fine for the optimizer, but a position loss would likely be imminent.

B. Position and velocity contraint handling

Expressions (17), (18) are used to estimate ν_e and η_e in (24), (25). Ideally one would want to fulfill the constraints continuously during the entire period δt during which the solution is to be applied on the vessel, but in practice it is sufficient to evaluate them at the end of this period. This choice admits the possibility that constraints would be violated during this period. The calculation for ν_e in (11) integrates over a constant term from T to T_e. This means that if the constraint (24) is not violated at either T or T_e, it can not be violated between T and T_e. This does not apply to the position constraint (25) since (12) integrates over velocity, but this violation will not be large enough to be practically significant since δt is typically too small to allow significant changes in the velocity of the ship during that period.

Due to the short horizon, when the constraints (24), (25) are approached, avoiding violation in the next time step could either be infeasible or would require too much energy. In a practical implementation, the constraints (24), (25) are replaced with a heuristically chosen cost term which is to be added to (23):

$$J_{\nu,\eta} = \|K_p \hat{\nu}_{e,T_e}\|_{Q_J}^2 + \|K_i \hat{\eta}_{e,T_e}\|_{Q_J}^2 \tag{29}$$

where Q_J is a weighing matrix to ensure prioritization between the degrees of freedom, while K_p and K_i are scalar constants. The effect of the factors K_p and K_i is analogous to the gains in the PI controller, although the relationship to the controller output is not linear.

C. Power feedforward

The feedforward request of power consumption increase or decrease rate $\dot{P}_{ff}$ is one of the goals for the thrust allocation algorithm. Preferably, the rate of change in the power consumption by the thrusters $\dot{P}_{th}$ should always match $\dot{P}_{ff}$, which implies a constant load on the power plant. This is of course not possible, so a near match most of the time is the actual goal of the thrust allocation algorithm. Both of those derivatives, as well as $\dot{f}$, should be calculated by discretization; forward Euler was used by the authors for testing purposes, i.e. $\dot{f} \approx {}^{f(T)-f(T-\delta t)}/_{\delta t}$. Notice that $f(T) = f$ is the decision variable, while $f(T - \delta t)$ is a constant parameter, equal to $f(T)$ from the previous iteration of the algorithm.

The power feedforward term P_{ff} signals a "soft" requirement for thrust allocation to increase or decrease its power consumption compared to power consumption in the previous iteration. Two applications for this signal may be considered. One use is to stabilize network frequency by setting it to

$$\dot{P}_{ff} = -k_{gp}(\omega_g - \omega_{0g}) \tag{30}$$

where k_{gp} is a positive constant, and $\omega_g - \omega_{0g}$ is the difference between the actual and the desired network frequency. A similar control strategy is employed in [10] on the level of the local thruster controllers. The other way to use this signal is to compensate for other power consumers that vary their consumption in a way that can be known in advance. The signal $\dot{P}_{ff}$ is used to reduce variations in the total power consumption by setting

$$\dot{P}_{ff} = -\dot{P}_{others} \tag{31}$$

where P_{others} is the power consumption by other consumers on the vessel. Since the power plant is able to handle rapid load reductions much better than rapid load increases, in this

paper the cost of load variation downwards is set to a fraction of load variation upwards, by changing the value of Θ in (23) depending on whether $\dot{P}_{th} - \dot{P}_{ff}$ is positive or negative.

D. Thruster biasing

To bias the thrusters is to deliberately increase the power consumption in the thrusters without changing the total produced force and moment on the ship, effectively forcing the thrusters to push against one another.

The combined force vector and angular momentum produced by the thrusters for a given azimuth and rudder angle vector α is given by (9),

$$\tau = B(\alpha)Kf \tag{32}$$

and is a linear combination of the forces f generated by the individual thrusters. If the ship is equipped with at least four thrusters, then the matrix $B(\alpha)K$ is guaranteed to have a non-trivial null space F_0. Additionally, if f^* is a strict global minimizer of the power consumption for a given τ, then for any $f_0 \in F_0 \setminus \mathbf{0}$ the power consumption for $f^* + f_0$ will be higher than for f^*, with the resultant generalized force remaining the same. Therefore, biasing can always be achieved as long as there are at least four non-saturated thrusters available for the purpose. Fewer than four thrusters are sufficient for configurations in which the columns of the matrix $B(\alpha)K$ are not independent.

Two practical applications for thruster biasing are discussed in this work: one is maintain a reserve capacity that the system can accept sudden load increases or power losses such as generator failures or short circuits of the part of the power system; the other one is to limit the rate of variations in load on the power plant.

1) Bias to keep a reserve capacity: Depending on the DP class, a DP vessel may be required to be able to continue operation uninterrupted after any single fault in the equipment. A typical worst case fault to be considered is a sudden disconnection of a single generator set or a single switchboard from the grid. Barring an emergency power source, this implies that at least two generator sets and switchboards must be operating at all times.

A marine diesel engine is unable to accept rapid load increases above a certain limit, mainly due to the time required to build up the pressure in the turbocharging system. A blackout can only be prevented if the load step on the remaining generators after the fast load reduction (FLR) system is activated does not exceed the load step capacity of the remaining diesel engines, also assuming that the FLR is able to reduce the load before the frequency variation tolerance is exceeded [22, p. 12]. It is up to the power management system to avoid the condition where a single fault may lead to blackout, which it can do by bringing more generator sets online so that a load step can be distributed between more engines. This can be done either by pre-calculated load-dependent start tables as in [23], or based on real-time worst-case scenario calculations as in [24].

Starting additional generators increases the wear-and-tear on the system. Also, when diesel engines are loaded far below their rated capacity, they are quite inefficient both in terms of specific fuel consumption and emissions. Biasing thrusters and allowing the FLR to release the bias when needed may allow the power plant to run with fewer generator online, which may be enough to compensate for the energy that is wasted in biasing. Consider for example a situation where a ship is equipped with a number of similar generators, each is able to accept a rapid load increse of 30% of its rated capacity. Due to calm weather, the power demand could be satisfied by running just one generator at 90% of its full capacity. The ship is performing a safety-critical operation, so it is an absolute requirement that a failure of one generator must not lead to blackout. As shown in Table IV, the vessel can operate safely by either having three geenrators online, or having two generators online and applying a bias equivalent to 30% of a generator's rated capacity. For the sake of simplicity, this example does not consider that FLR will typically attempt to assist the remaining generators by disconnect non-essential consumers from the grid; this capability is helpful, but often not sufficient.

This approach is extensively applied in the industry, among others by Kongsberg, and is mentioned in publications such as [13], [25], [26]. A contribution of the present work is a fairly general formulation of thruster biasing for the purpose of keeping a power reserve in the optimization problem.

2) Bias to cushion load drops: As discussed previously, sharp decreases in power consumption may affect the power plant negatively. Therefore, it makes sense to even out load decreases by burning off some of the energy. This obviously incurs costs in terms of fuel consumption and in many cases in wear-and-tear on the thruster units. The proposed thrust allocation algorithm automatically weighs those costs against the benefits, and biases the thrusters if this is optimal.

3) Force variation: Because of the bias, the second cost term in (23), $\left\|K\dot{f}\right\|_{\Psi}^2$, is necessary because the addition of the constraint (27) can otherwise under some circumstances turn the solution of (23)–(28) into a continuous set with an infinite number of solutions. Without (27) , a specific thruster command f will be a global minimizer of the optimization problem. However, the bias request can typically be achieved by addition to f of any permutation f_0 from a continuous set – and all of them may minimize (23) without $\left\|K\dot{f}\right\|_{\Psi}^2$. The third term, $\Theta\left(\dot{P}_{th} - \dot{P}_{ff}\right)^2$, helps the situation a little because it attempts to drive $\dot{P}_{th} = P_c K \left|\dot{f}\right|^{3/2}$ towards a specific value. It is however at best one equality for N (number of thrusters) degrees of freedom, so the solution set f may not always be a point.

With many numerical solvers, this would lead to chatter in the output. This complication can be illustrated on a simplified problem

$$\min_x \frac{1}{2}x^T G x \tag{33}$$

subject to

Generators online	Biasing	Load per generator	Load per generator after a single generator failure	Blackout preventable
1	No	90%	N/A	No
2	No	45%	90%	No
3	No	30%	45%	Yes
2	Yes	60%	90%	Yes

TABLE IV: A scenario showing that a marine power plant may sometimes safely run with fewer generators online if some energy is wasted by biasing the thrusers. The power demand is equal to 90% of the capacity of one generator.

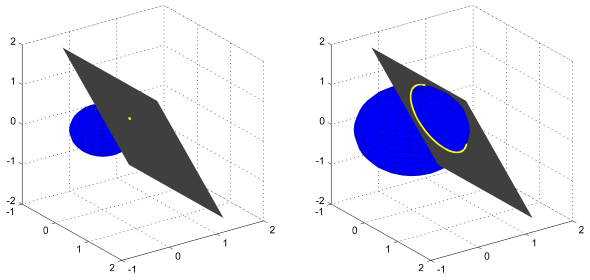

(a) For $z_{min} = z^*_{min}$, the solution set is a point.

(b) For $z_{min} > z^*_{min}$, the solution set is a circle.

Fig. 5: The set of solutions of the simplified optimization problem (33)–(35) with $N = 3,\ M = 1$ shown in yellow. If the second problem were to be used in optimization-based control, the output of the controller would likely vary a lot between the samples. The original problem (23)–(28) would exhibit a similar structure without the cost on time derivative of the individual thruster outputs f.

$$Ax = b \tag{34}$$

$$\frac{1}{2}x^T Gx \geq z_{min} \tag{35}$$

where $G \in \mathbb{R}^{N\times N}$, $A \in \mathbb{R}^{M\times N}$ are matrices of full rank with $N \geq M + 2$, and z_{min} a scalar which is larger than the global minimum z^*_{min} of this optimization problem without the constraint (35). The solution to this problem is a connected set. For $N = 3,\ M = 1$ this is illustrated on Figure 5. If the left hand side of (35) is not identical to the cost function but instead a slight permutation of it, the solution of the optimization problem would in general be unique, but sensitive to changes in the permutation between the iterations, which would also result in chatter.

V. Simulation – Case Study

The proposed thrust allocation algorithm was tested in a simulation, on a model of SV Northern Clipper, featured in [18].

A model of a diesel-electric power plant was developed as part of this work. It is introduced in Subsection V-D, with implementational details left out for Appendix A.

A. Hull and thruster system

The simulated vessel is 76.20 meters long, with a mass of $4.591 \cdot 10^6$ kg. It has four thrusters, with two tunnel thrusters near the bow and two azimuth thrusters at the stern. The maximal force for each thruster was set to $1/60$ of the ship's dry weight.

Fig. 6: Thruster system on the simulated ship.

The ship is illustrated in Figure 6.

B. Motion control algorithm

The applied high-level motion control algorithm is a set of three PID controllers, one for each degree of freedom.

C. Power plant and distribution

The power plant installed on the simulated vessel consists of three generator sets. Two of them are rated at 1125 kVA, and the third one at 538 kVA. All gensets are connected to a single distribution bus. The engine governors were set in droop mode with the setpoint frequency of 60 Hz and a 5% droop. This power plant is sufficiently complex for testing control principles. It is more complex than the illustration in Figure 1, but still much simpler than found on most practical vessels.

The power management system supplied a feed-forward signal to the thrust allocation algorithm per (31).

D. Diesel engine model

In this subsection, the main principles of modeling of a marine diesel engine are discussed, with implementational details left for Appendix A.

A very accurate model for a turbocharged diesel engine can be constructed using a CFD simulation of the process fluids in the engine combined with a model of the dynamic behavior of the mechanical parts throughout the combustion cycles. Less accurate but more practical cycle-mean quasi-steady models, such as those examined in [27]–[29], are capable of reasonable quantitative prediction of the diesel engine behavior on the time scales comparable to a drive shaft revolution.

A diesel engine deployed in a power plant is controlled by its governor in a tight feedback loop, which counteracts much of the dynamic behavior of the engine. The scope of this work is not a detailed investigation of the dynamic response of a particular diesel engine, but rather a more general

performance testing of the power grid as a whole. The model of the diesel engine needs to accurately represent the most important dynamical properties of the engine as well as the physical limitations which are impossible for the governor to correct. The most important such limitation is the turbocharger lag, which limits the amount of oxidizer in the cylinders, and therefore also the maximum effective fuel injection. Other practically important factors include the fuel index rate limit, and a governor response lag. The latter is an inevitable factor in feedback-based governors, since they cannot undertake any correcting action until after a deviation from the velocity setpoint is measured, and the aggressiveness of that correcting action is usually limited by stability considerations.

The authors could not find a fitting model in the literature, so a model was developed in [14], and is included in Appendix A for completeness. It is based on [27], [30]–[32], being a simplification of the model in [27]. The same model was used in [33] as a prediction model for an MPC governor.

The benefit of this model compared to other models in the literature is that situations when the engine experiences large load variations are represented with a reasonable degree of fidelity, while in most other respects the model remains fairly simple.

From the practical perspective, this model does not include a rate limiter, and therefore permits load variations that are so large that they would quickly wear down the engine due to thermic variations. The marine diesel engine manufacturers typically limit the permitted rate of change of the fuel index, both upwards and downwards. The thrust allocation algorithm presented in this work attempts to keep the variations in load on the power plant as low as possible, and there is no reason to push them lower than that.

If the EGR (exhaust gas recycling) is installed on the engine, it is assumed to be reduced or disabled during the upward transients.

E. Diesel engine governor

A diesel engine prime mover for a power plant has to maintain its rotational velocity in presence of variations in the load. This requires a feedback-based controller. The controllers for the diesel engines are conventionally called “governors”. Ill-designed governors may create unnecessary variations in the electric frequency, increase fuel consumption on the grid and in the worst scenarios destabilize the plant. Legacy implementations are either distributed droop governors, or isochronous governors. Droop governors are usually implemented as PID controllers that measure the deviation in the electric frequency from a drooped setpoint and control the fuel index accordingly. Isochronous governors have a constant (non-drooped) frequency setpoint but also share information about the average load on each connected bus segment through a separate load sharing line. Introductory texts about marine diesel control systems are available in e.g. [30], [34], [35], and [2, sec 4.4.1]. More modern control methods for marine power plants, such as those in the recent Kongsberg power management systems, use droop-based governors but rapidly modify the droop curve based on the loading situation. This way, they achieve both the fault tolerance of the droop governors and the frequency stability of the isochronous governors.

The governor used in conjunction with this thrust allocation algorithm is a droop governor, with a functionality for feedforward from the loads. The proposed feedforward implementation measures the total electric load, distributes it between the available generator sets, calculates the approximate fuel index which would produce the electric power currently consumed, and adds this value to the output of the PID controller. This way, when the power consumption changes, the fuel index rapidly changes to a value close to what is needed to match the produced mechanical power and the consumed electrical power. With these nearly balancing each other out, the torques on the rotating parts of the generating set will approximately match, resulting in a near-constant rotational velocity. The remaining deviation is due to modeling inaccuracies and will be corrected by the PID controller. In a practical implementation, the output from the feedforward could be passed through a low-pass filter to avoid excessive fuel index movement.

Tests were conducted both with and without the feedforward. Without the feedforward, a droop governor can only respond to changes in load after these changes affect the frequency. This leads to frequency variations that do not originate in the physical limitations of the system.

This architecture bears a certain resemblance to an isochronous controller since the feedforward term is similar to the value on the load sharing line. However, the value on the load sharing line in an isochronous governor is passed through the PID of the governor, which does not appear to be necessary.

As mentioned in Subsection V-D, the density of the air injected into the cylinders limits how much fuel can be effectively injected into the cylinder. It is assumed that the diesel engine fuel limiter informs the governor about the maximum efficient fuel index, and the governor is never allowed to exceed this value.

The introduced thrust allocation algorithm reduces the load variations in the network essentially by delaying some of the power consumption. In situations with large and rapid load increases, this results in the governor first reacting less than it would have with a standard thrust allocation algorithm, for instance the one described by (19)–(21). Afterwards it is unable to move the fuel index enough to deliver power for the delayed consumption due to the limitations mentioned above. In simulation tests, this situation often resulted in unnecessarily large frequency drops. To avoid this, the feedforward implementation was modified to use the information of the power the thrust allocation would have used if it had fulfilled the command exactly, i.e., P_{min} from (19) is distributed to the governors. Since an amount similar to that difference is likely to be requested by the thrusters shortly, it is prudent for the governor to prepare for the coming load increase. In this paper, this was done by integrating the power difference in time to acquire an energy quantity, and changing the setpoint frequency so that the resulting change in the kinetic energy of the rotating machinery would be equivalent to the energy difference produced by the thrust allocation algorithm.

F. Adaption for a split bus tie configuration

The algorithm was only tested on a fully connected bus. It could be adopted to a split bus configuration by using a separate power feedforward term $\Theta\left(\dot{P}_{th} - \dot{P}_{ff}\right)^2$ in the cost function (23) for each of the bus segments. Similarly, the biasing and power limit constraint (27) has to be applied individually for each of the bus segments.

G. Simulation results

The simulation was implemented in Simulink, and the Matlab Optimization Toolbox was used to solve the numerical optimization problem. The update frequency for thrust allocation was set to 0.2 seconds. The simulation was run on a laptop computer with an Intel i7 Q820 CPU.

Five configurations were tested with different combinations of options, as presented in Table V. In the first configuration, the governors were run with feedback-only control and a classical droop implementation, and no attempt by the thrust allocation algorithm to reduce the load variations. In the second simulation, the governors received a feedforward from the loads, but again with no assistance from the thrust allocation. The first and the second configurations functioned as a baseline to evaluate the effect of the proposed features in the thrust allocation algorithm. In the third configuration, the thrust allocation introduced counter-acting load variations as proposed in this paper. A stochastic disturbance representing environmental disturbances that were not compensated by the wind feedforward or wave filter [17] was added in simulations four and five.

The initial position in the simulations is two meters away from the setpoint in surge. None of the five test cases included an initial deviation in sway or heading. A constant environmental (wind) force from the stern of the vessel equivalent to 2% of the ship's weight, that is $\begin{bmatrix} 0.02 & 0 & 0 \end{bmatrix}^T$ in the bis system normalization [17, table 7.2] was present in all simulation cases. Since the initial deviation is in the direction of surge only and the environmental disturbance is deterministic and acts strictly in the same direction, very little deviation in those degrees of freedom was observed in the simulation. This configuration was selected to make the power-related features of the algorithm easier to interpret. The algorithm controls the position of the vessel in 3 DOFs, and is successfully rejecting disturbances in test cases 3–5. The azimuth thrusters are oriented 45 degrees towards the center line of the the ship. Since the presented thrust allocation algorithm does not include methods for rotating those thrusters, they remain at that orientation for the entire course of the simulation.

In addition to the thrusters, a periodic, fast-rising load of $1.5\,\mathrm{MW}$ was present on the grid to emulate the load from a heave-compensated platform or a similar wave-induced load typical for a drilling vessel. This load stays at $1.5\,\mathrm{MW}$ for two seconds before subsiding to $0.2\,\mathrm{MW}$ where it stays for additional two seconds, after which it drops to zero. The fuel rate limiters were not enabled on the governors. The tolerances for deviation in position were set to 1 meter in each direction, while the tolerances in deviation in velocity were set to 0.3 m/s. The weight factors in (29) were set such that deviation in either $\hat{\nu}_{e,\,T_e}$ or $\hat{\eta}_{e,\,T_e}$ equal the respective tolerances would incur a cost equivalent to all thrusters running at full power. The cost of power variations downwards was set to be very low in order to avoid increased specific fuel consumption compared to the base scenarios. Most other configuration parameters were set by trial and error.

Figure 7 shows the total load on the bus in the first three test cases. In the first two, the thrusters don't do anything except compensating for the slowly-varying environmental force. Because of that, their load does not vary a lot, and the periodic $1.5\,\mathrm{MW}$ load enters the power plant unhindered. In the third case, when the thrust allocation algorithm power control is activated, the total load variations are significantly more smooth.

The modified thrust allocation algorithm informs the governors that it is delaying power consumption. As shown on Figure 9, this gives the governors time to increase the power production, as well as accelerate the turbocharger shaft and increase the pressure in the scavenging receiver. This initially leads to an increase in frequency, resulting in a slight overfrequency but also some additional energy being stored in the rotating masses. The resulting frequency variations are displayed in Figure 8. Had the fuel index rate limiter been activated, this would instead lead to a lower mismatch between generated and consumed energy, and therefore lower frequency deviation.

Without the feedforward from the loads, an abrupt change in load leads to a change in the frequency setpoint due to the droop. This is a fundamental limitation of the droop governors, because during a load transient, a local governor does not have enough information to determine if e.g. a load increase it observes on it own terminals is due to an increase in the load on the bus or due to it having taken a larger share of the load from the other generators. Those conditions require opposite actions, and it is not possible to determine which is correct until the frequency on the grid decreases due to the increased load. This is less of an issue in isochronous mode since a load increase does not lead to a setpoint frequency drop, but the governor still have to wait until it observes a frequency deviation until it can change the position of the fuel index.

The position of the vessel in surge for test cases 1–3 is shown in Figure 10. Use of the proposed thrust allocation algorithm leads to small variations being superimposed on the trajectory of the vessel, which in this simulation are well within required precision for most offshore operations. The largest acceleration the ship experiences during the simulation is $0.11\,\mathrm{m/s^2}$. This happens during the initial setpoint acquiring, and it is not related to the load variation compensation features of the algorithm. For this reason there will be no deviation in those directions in test cases 1–3, and the respective plots are omitted. This scenario was selected to make the power-related effects more emphasized – returning a ship to the setpoint from any desired starting point is not a new challenge, and the proposed algorithm does not behave differently from other algorithms in the literature in that regard.

Deviation in sway and in yaw (the latter being rather small) were present when a random component was added to the environmental forces. The main motivation for adding the

Simulation case	Governor feedforward	TA power modulation	Uncompensated environmental disturbances
1	no	no	no
2	active	no	no
3	active	active	no
4	active	active	yes
5	no	no	yes

TABLE V: Tested configurations

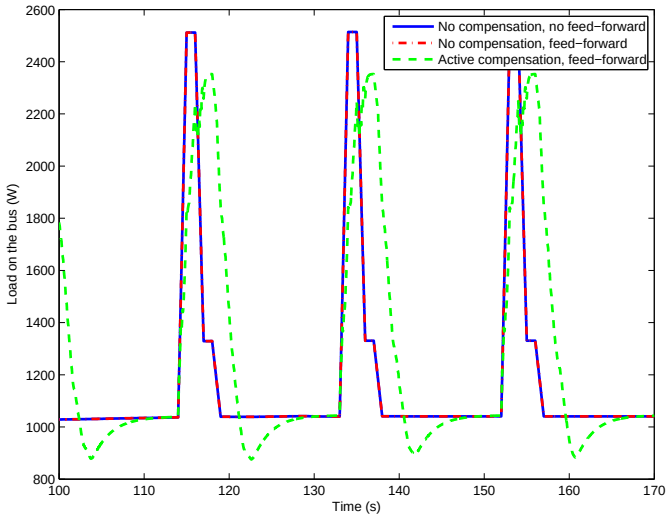

Fig. 7: Total load; test cases 1, 2, 3

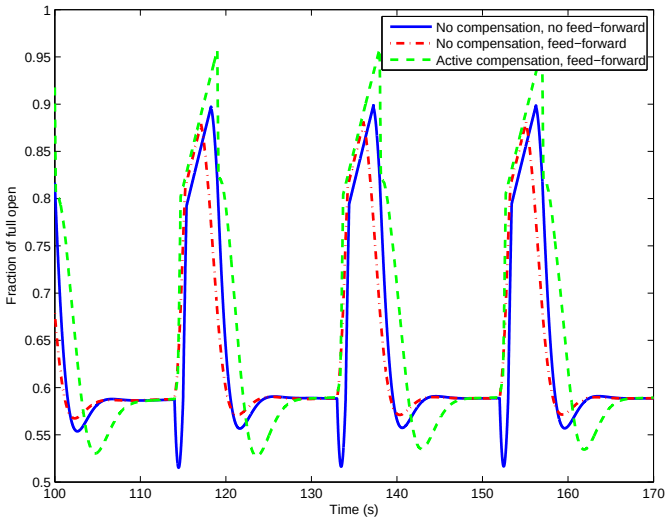

Fig. 9: Fuel injection rate on one of the generators; test cases 1, 2, 3

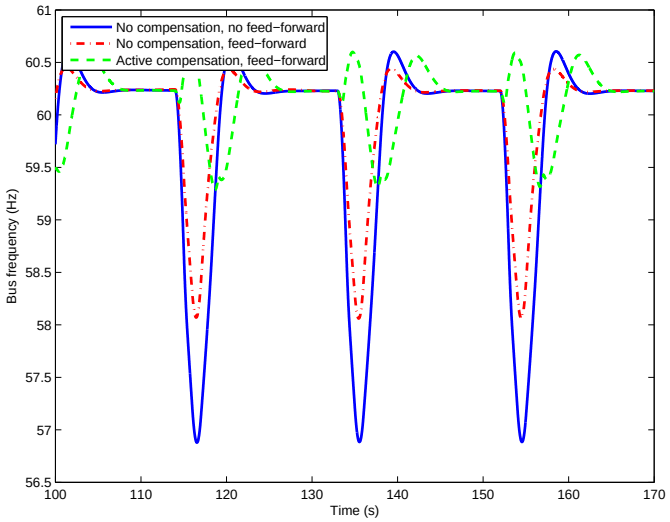

Fig. 8: Bus frequency; test cases 1, 2, 3

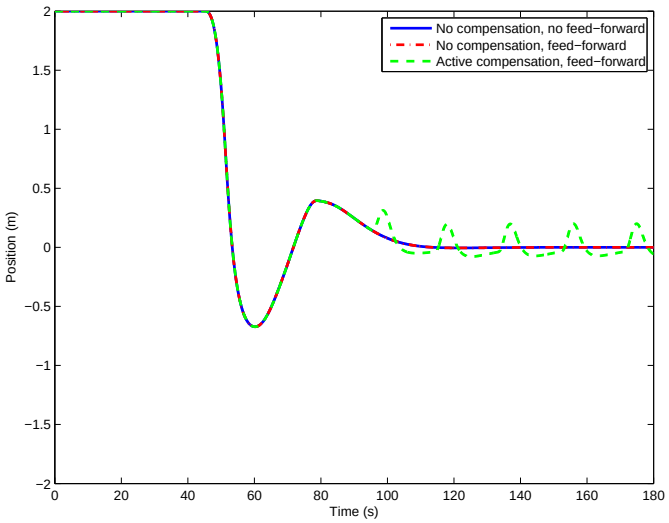

Fig. 10: Position of the vessel in surge; test cases 1, 2, 3

random component to the environmental force is the fact that the environmental forces are not deterministic in reality. The position of the vessel in surge with and without the random environmental disturbances is shown in Figure 11. It shows that the disturbances due to the thrust allocation PMS assistance are not large compared to typical random disturbances. The effect of the thrust allocation algorithm modification on the frequency is not qualitatively affected by the random disturbances, as shown on Figure 14.

VI. Discussion and Conclusion

The proposed thrust allocation algorithm has been demonstrated to reduce load variations on a marine power plant by making the thrusters produce counteracting load variations that partially cancel the load variations from the other consumers. This can be taken advantage of either through reducing frequency variations as has been demonstrated in simulation, or alternatively by reducing the variations in the fuel index, thus reducing wear-and-tear on the engine, emissions and sooting.

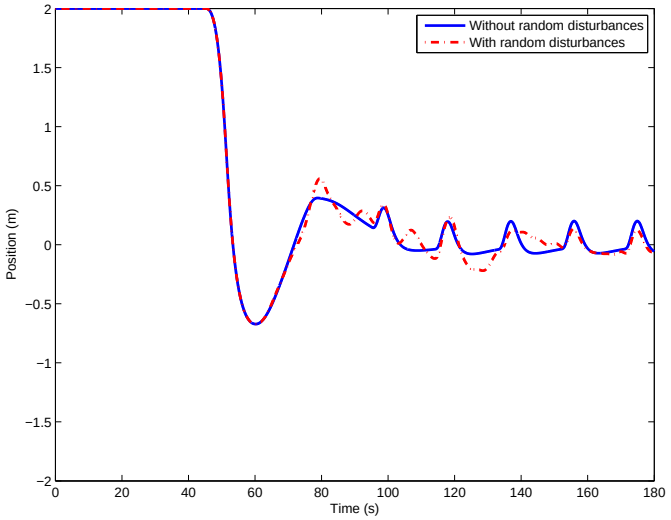

Fig. 11: Position of the vessel in surge with and without uncompensated environmental disturbances, with PMS assistance activated; test cases 3, 4

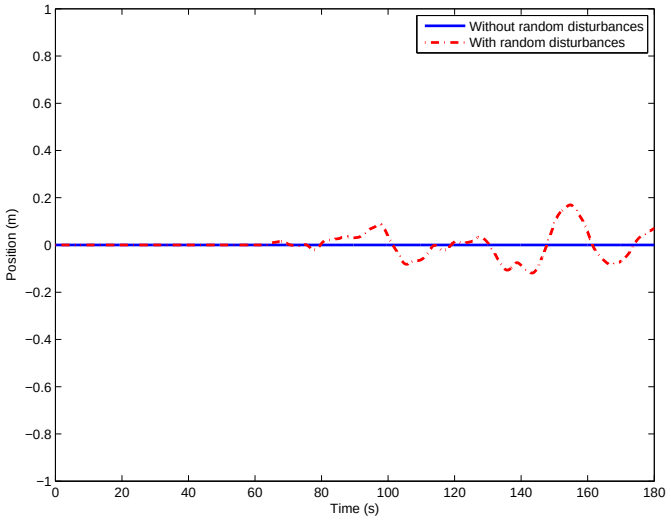

Fig. 12: Position of the vessel in sway with and without uncompensated environmental disturbances, with PMS assistance activated, repositioning deactivated; test cases 3, 4

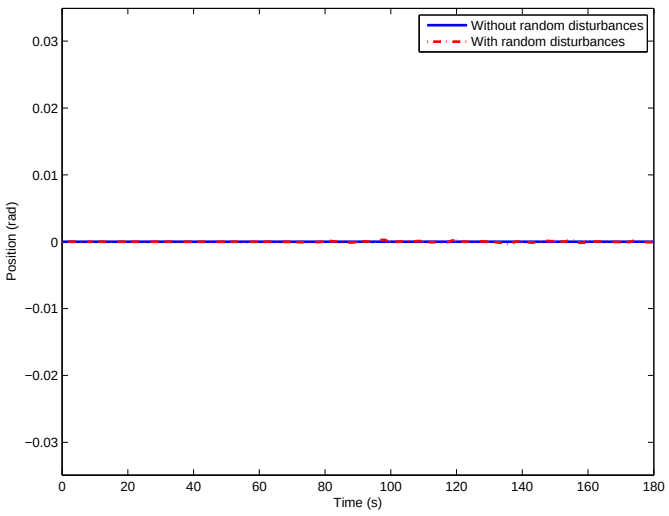

Fig. 13: Orientation of the vessel in yaw with and without uncompensated environmental disturbances, with PMS assistance activated, repositioning deactivated; test cases 3, 4

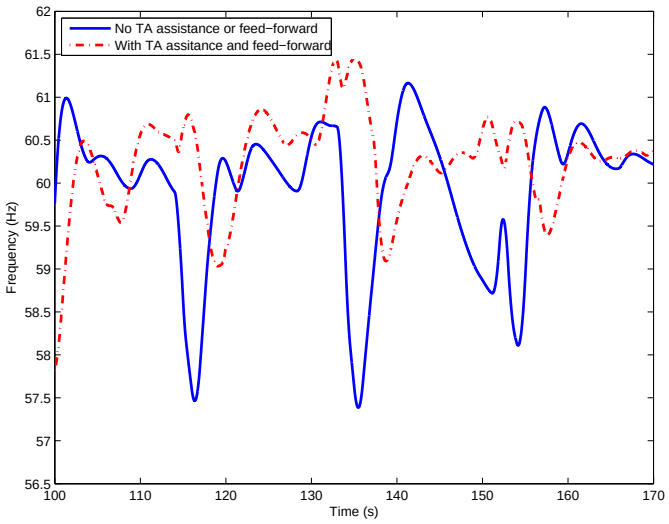

Fig. 14: Frequency on the grid with uncompensated environmental disturbances; test cases 4, 5

The optimization is done with regards to the current state only, so the response may not be optimal with regards to how the load continues to evolve. For example if there is a load increase, the algorithm has no way of knowing if it is a very short load peak or a load step. If the former is the case it would have been preferable to allow the ship to mostly drift while the load peak lasts, and then slowly bring the ship back to the setpoint position. If the latter is the case, then it is more optimal to "spread out" the load reduction in the thrusters over a longer period of time to allow a smoother load increase.

The algorithm was tested in fairly realistic conditions, which resulted in some practical challenges. In particular, tuning of the algorithm was time-consuming. The cost terms in (23) and in (29) have to be carefully balanced against each other to ensure that the thrust allocation does not respond to the load variations elsewhere too aggressively or too calmly. If the controller responds too aggressively, it would "spend" its position margin too quickly, and fail to reduce load peaks for the largest loads. If it responds too calmly, then this algorithm will effectively no longer consider introducing position deviations to compensate for load variation. This situation is not untypical, as marine control systems are in general difficult to tune for a wide range of operational scenarios. The proposed algorithm does however add a layer of complexity to the control system.

REFERENCES

[1] *Rules for classification of ships*, DNV GL STD. PART 6 CHAPTER 7, DYNAMIC POSITIONING SYSTEMS, JULY 2013.

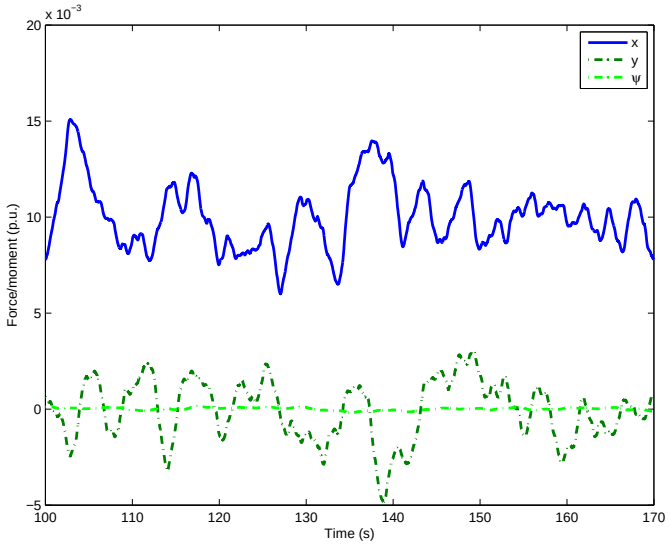

Fig. 15: Environmental disturbances, including random uncompensated disturbances; test case 4 (test case 5 is qualitatively similar but driven by a different random noise realization)

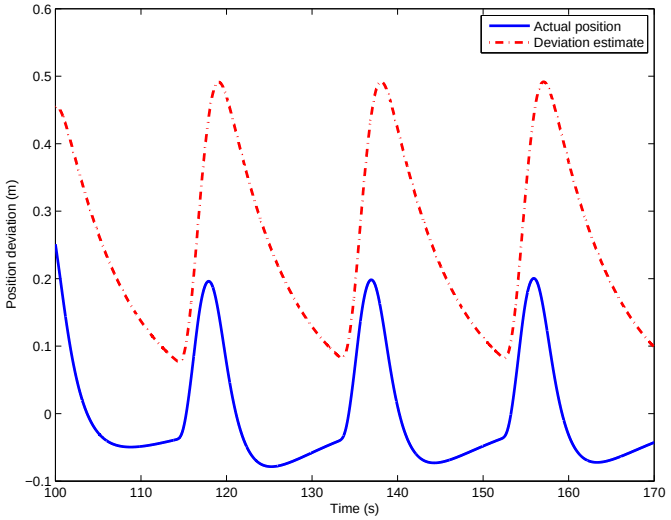

Fig. 16: Position deviation estimate in surge due to effects of the thrust allocation deviations, superpositioned on the actual position shows the interaction between the dynamic positioning algorithm and the deviation in thrust allocation; test case 3

[2] A. K. Ådnanes, "Maritime electrical installations and diesel electric propulsion," ABB AS, Tech. Rep., 2003.

[3] P. Lakshminarayanan and Y. V. Aghav, *Modeling Diesel Combustion*, F. F. Ling, Ed. Springer, 2009.

[4] P. Eckert and S. Rakowski, *Combustion Engines Development*. Springer-Verlag, 2012, ch. Pollutant Formation.

[5] C. D. Rakopoulos and E. G. Giakoumis, *Diesel Engine Transient Operation*. Springer, 2009.

[6] T. A. Johansen, T. P. Fuglseth, P. Tøndel, and T. I. Fossen, "Optimal constrained control allocation in marine surface vessels with rudders," *Control Engineering Practice*, vol. 16, no. 4, pp. 457 – 464, 2008.

[7] N. A. Jenssen and B. Realfsen, "Power optimal thrust allocation," in *MTS Dynamic Positioning Conference*, Houston, 2006.

[8] T. A. Johansen, T. I. Fossen, and S. P. Berge, "Constrained nonlinear control allocation with singularity avoidance using sequential quadratic programming," *IEEE Trans. Control Systems Technology*, vol. 12, pp. 211–216, 2004.

[9] T. A. Johansen, T. I. Bø, E. Mathiesen, A. Veksler, and A. Sørensen, "Dynamic positioning system as dynamic energy storage on diesel-electric ships," *IEEE Transactions on Power Systems*, 2014, (in press).

[10] D. Radan, A. J. Sørensen, A. K. Ådnanes, and T. A. Johansen, "Reducing power load fluctuations on ships using power redistribution control," *SNAME Journal of Marine Technology*, vol. 45, pp. 162–174, 2008.

[11] E. Mathiesen, B. Realfsen, and M. Breivik, "Methods for reducing frequency and voltage variations on DP vessels," in *MTS Dynamic Positioning Conference*, Houston, October 2012.

[12] T. A. Johansen and T. I. Fossen, "Control allocation – a survey," *Automatica*, vol. 49, no. 5, pp. 1087 – 1103, 2013.

[13] A. Veksler, T. A. Johansen, and R. Skjetne, "Thrust allocation with power management functionality on dynamically positioned vessels," in *Proc. American Control Conf.*, 2012.

[14] ——, "Transient power control in dynamic positioning-governor feedforward and dynamic thrust allocation," in *9th IFAC Conference on Manoeuvring and Control of Marine Craft*, 2012.

[15] L. Pivano, T. A. Johansen, and . N. Smogeli, "A four-quadrant thrust estimation scheme for marine propellers: Theory and experiments," *A Four-Quadrant Thrust Controller for Marine Propellers with Loss Estimation and Anti-Spin: Theory and Experiments*, vol. 17, pp. 215–226, 2009.

[16] P. Maciel, A. Koop, and G. Vaz, "Modelling thruster-hull interaction with cfd," in *32nd International Conference on Ocean, Offshore and Arctic Engineering, Nantes, France.*, June 2013.

[17] T. I. Fossen, *Handbook of Marine Craft Hydrodynamics and Motion Control*, April 2011.

[18] ——, *Marine Control Systems*. Tapir Trykkeri, 2002.

[19] O. M. Faltinsen, *Hydrodynamics of High-Speed Marine Vehicles*. Cambridge University Press, 2006.

[20] C. Holden, "Modelling and control of parametric roll resonance," Ph.D. dissertation, NTNU, June 2011.

[21] *Nomenclature for Treating the Motion of a Submerged Body Through a Fluid*, Technical and Research Bulletin No. 1-5, The Society of Naval Architects and Marine Engineers, Technical and Research Committee Std., 1950.

[22] D. Radan, "Integrated control of marine electrical power systems," Ph.D. dissertation, NTNU, 2008.

[23] D. Radan, T. A. Johansen, A. J. Sørensen, and A. K. Ådnanes, "Optimization of load dependent start tables in marine power management systems with blackout prevention," *WSEAS Trans. Circuits and Systems*, vol. 4, 2005.

[24] T. I. Bø and T. A. Johansen, "Scenario based fault tolerant model predictive control for diesel-electric marine power plant," in *Proc. MTS/IEEE OCEANS*, 2013.

[25] S. Savoy, "Ensco 7500 power management system design, functionality and testing," in *MTS Dynamic Positioning Conference*, 2002.

[26] X. Shi, Y. Wei, J. Ning, M. Fu, and D. Zhao, "Optimizing adaptive thrust allocation based on group biasing method for ship dynamic positioning," in *Proceeding of the IEEE International Conference on Automation and Logistics, Chongqing, China*, 2011.

[27] N. Xiros, *Robust Control of Diesel Ship Propulsion*. Springer-Verlag, 2002.

[28] G. Theotokatos, "A comparative study on mean value modelling of two-stroke marine diesel engine," in *Proceedings of the 2nd International Conference on Maritime and Naval Science and Engineering*. World Scientific and Engineering Academy and Society, 2009, pp. 107–112.

[29] ——, "Ship propulsion plant transient response investigation using a mean value engine model," *International Journal Of Energy*, vol. 2, no. 4, pp. 66–74, 2008.

[30] R. Skjetne, "Modeling a diesel-generator power plant," Lecture notes in course TMR4290, 2011, NTNU, October 2011.

[31] I. Boldea, *Synchronous Generators*. CRC Press, November 2005.

[32] S. ROY, O. MALIK, AND G. HOPE, "ADAPTIVE CONTROL OF SPEED AND EQUIVALENCE RATIO DYNAMICS OF A DIESEL DRIVEN POWER-PLANT," *IEEE Transactions on Energy Conversion*, VOL. 8, NO. 1, PP. 13 –19, MAR 1993.
[33] A. VEKSLER, T. A. JOHANSEN, E. MATHIESEN, AND R. SKJETNE, "GOVERNOR PRINCIPLE FOR INCREASED SAFETY AND ECONOMY ON VESSELS WITH DIESEL-ELECTRIC PROPULSION," IN *Proc. European Control Conf.*, 2013.
[34] T. I. BØ, "DYNAMIC MODEL PREDICTIVE CONTROL FOR LOAD SHARING IN ELECTRIC POWER PLANTS FOR SHIPS," MASTER'S THESIS, NTNU, 2012.
[35] *Governing Fundamentals and Power Management*, 2620TH ED., WOODWARD, 2004.
[36] *TCA - The Benchmark*, MAN DIESEL & TURBO, 86224 AUGSBURG, GERMANY, 2013.

APPENDIX A
MODELING OF THE DIESEL PRIME MOVER

The intended area of application for this marine diesel engine model is in design and testing of control systems for marine power plants. It is intended to be general enough to be easily configurable, but still describe the engine both under relatively low load variations that are expected during normal operations, and during extreme load variations when the engine would be asked to deliver as much power as it is physically able.

A. Assumptions and simplifications

Compared to the model in [27], the following assumptions and simplifications are made in this model:

- The angular velocity of the turbine is assumed to depend on the generated power only. In reality this relationship is quite dynamic, with other factors such as thermodynamic relationships incorporated in the exhaust manifold. Still, both generated power and the exhaust volume that drives the turbocharger depend upon how much fuel is burned per unit of time, and both relationships are linear to some degree.
- To calculate the Air-to-Fuel ratio (AF) after each injection, it is assumed that the fuel injected into the cylinder in each cycle is proportional to the fuel index position. The amount of air entering the cylinder is assumed to be linearly dependent on the velocity of the turbocharger compressor. If the compressor velocity is zero, then the amount of air entering will be $m_{a,0}$, and it will linearly increase to a maximum value as the velocity of the compressor approaches its maximum value.
- There is a delay in the order of $(60/N) \cdot (2/z_c)$ seconds from fuel index change until the corresponding change of torque on the drive shaft. The main cause of the delay is that it takes time before the new measure of fuel is injected into the next cylinder in the firing sequence, and in addition it takes some more time before the ignition leads to increased in-cylinder pressure and then increased torque on the drive shaft [5, p. 25]. The nominal RPM of the engines in the simulation was around $N = 1800$, so this delay had little practical consequence and was ignored.
- On older engines, setting a new value for the fuel index involved moving an actual fuel rack, a mechanical device which determined the fuel injection rate into the engine, resulting in a certain amount of lag. On newer engines with direct fuel injection there is no physical fuel rack, so this delay is not included in the model.
- Performance of a diesel engine during a large transient is limited by the performance of the turbocharger, which needs time to increase the pressure in the intake manifold. Until it does, the concentration of oxygen in the combustion chamber will limit the combustion.
- The damping due to friction is mostly a function of the current engine RPM. Since the engine in a power plant normally operates in a narrow RPM range, this friction is not important for the dynamical performance of the engine and was not modeled.

B. Variables

The variables used for the diesel engine model are described in Table VI.

Symbol	*Description*
p_e	Break mean effective pressure in the cylinders (p.u.)
t_m	Total mechanical torque from an engine (p.u.)
t_e	Electrical torque (p.u.)
$p_{e,r}$	Rated BMEP (Pa)
N	Instantaneous crank shaft RPM
N_r	Nominal engine RPM
z_c	Number of cylinders
V_h	Cylinder volume (m^3)
η_c	Combustion efficiency (non-dimensional, p.u.)
F_r	Fuel rack/fuel index position (nondimensional, p.u.), which determines the amount of fuel injected into the combustion cylinders per diesel cycle.
ω_t	Turbocharger rotational velocity (p.u.)
T_t	Turbocharger dynamics time constant
$m_{a,0}$	Air flow (mass) without the turbocharger as fraction of the maximal airflow
AF_n	Nominal air-to-fuel ratio on max turbocharger velocity and max BMEP
AF_{low}	Air-to-fuel ratio at which the combustion stops due to excessive in-cylinder cooling from the injected fuel.
AF_{high}	Air-to-fuel ratio at which full combustion is achieved. Typical values: 20-27 for HFO, 17-20 for Diesel Oil
P	Current engine power output (Watt)
P_l	Power consumed by the load (Watt)
P_r	Rated engine power (Watt)
I	Moment of inertia of the rotating mass in the genset ($\mathrm{kg} \cdot \mathrm{m}^2$)
H	Inertia constant of the engine, represented as the time needed for the engine running at nominal power to produce the energy equivalent to the kinetic energy in the rotating mass at nominal speed.

TABLE VI: Variables used for the diesel engine model.

C. Formulas

$$AF = \frac{m_{a,0} + (1 - m_{a,0})\omega_t}{F_r} \cdot AF_n \tag{36}$$

$$\eta_c = \begin{cases} 1 & AF \geq AF_{high} \\ \frac{AF - AF_{low}}{AF_{high} - AF_{low}} & AF_{low} < AF < AF_{high} \\ 0 & AF \leq AF_{low} \end{cases} \tag{37}$$

$$t_m = p_e = \eta_c F_r \tag{38}$$

$$\dot{\omega}_t = -1/T_t(\omega_t - p_e) \tag{39}$$

$$P = p_{e,r} p_e z_c V_h {}^N/_{60} = P_r t_m {}^N/_{N_r} \tag{40}$$

$$H = \frac{\frac{1}{2} I \left(\frac{2\pi N_r}{60}\right)^2}{P_r} \tag{41}$$

$$\dot{N} = \frac{\frac{1}{2} N_r (t_m - t_e)}{H} \tag{42}$$

The torque balance enters the swing equation in (42); the electrical torque t_e is an external input to this model and has to come from the model of the generator. The equation (39) is a rough representation of the turbocharger lag, which includes a large variation of effects, such as pressure buildup in the exhaust manifold (if the turbo is not pulse charged), acceleration of the turbocharger shaft and buildup of the pressure in the intake manifold, as well as heating up the engine to the new working temperature.

The fuel rack can change the fuel injection arbitrarily, which roughly translates to a change in BMEP (p_e in per-unit) after a short injection and combustion delay which may not be modeled. Since cycle-mean torque delivery is proportional to BMEP, the per-unit torque t_m has the same numerical value, as expressed in (38). If the turbocharger didn't have time to increase air delivery sufficiently, then either the combustion efficiency will be reduced as per (38), or the fuel rack limiter will be activated and not allow the fuel rack to exceed the maximal efficient value.

D. Numerical values

The parameters for the simulation are matched so that they represent a typical marine diesel engine of the size mentioned in section V-C. The stoichiometric ratios AF_* are taken within the range specified in [27, page 23], $AF_{high} = 20$, $AF_{low} = 14$. The air-to-fuel ratio under full power and fully developed turbocharger velocity is set to 27. The naturally perspired efficiency m_{a0} is set to 0.2 to reflect the compression ratio in the modern marine turbochargers, which is around 5 [36]. The losses in the conversion of power from the mechanical to electrical systems are not modeled, so the rated power P_r of each diesel engine can be calculated from the genset rated power as mentioned in section V-C.

APPENDIX B
ACKNOWLEDGMENTS

This work is partly sponsored by the Research Council of Norway by the KMB project D2V, project number 210670, and through the Centres of Excellence funding scheme, project number 223254 – AMOS. Eirik Mathiesen is employed with Kongsberg Maritime. Valuable comments that led to significant improvements of parts of the paper were contributed by Trond Toftevaag of SINTEF, Eilif Pedersen of NTNU, and Bjørnar Realfsen of Kongsberg.

Aleksander Veksler is a graduate student at the Institute of Engineering Cybernetics at the Norwegian University of Science and Technology (NTNU), Trondheim. He was born in 1982 and received his MSc in Engineering Cybernetics in 2009 from NTNU. He was a research visitor to UCSD in 2008/2009 while working on his Master's thesis.

Professor Tor A. Johansen was born in 1966, received his MSc degree in 1989 and Ph.D. degree in 1994, both in electrical and computer engineering from the Norwegian University of Science and Technology, Trondheim. He worked at SINTEF Electronics and Cybernetics as a researcher before he was appointed Associated Professor in Engineering Cybernetics at the Norwegian University of Science and Technology in Trondheim in 1997 and was promoted Professor in 2001. He was a research visitor at the USC, TU-Delft and UCSD. He has published more than 100 articles in international journals as well as numerous conference articles and book chapters in the areas of nonlinear control and estimation, optimization, adaptive control, and MPC with applications in the marine, automotive, biomedical and process industries. He has been supervising more than 10 PhD students, holds several patents, and has been directing numerous research projects. In December 2002 Johansen co-founded the company Marine Cybernetics AS where he was Vice President until 2008. Prof. Johansen received the 2006 Arch T. Colwell Merit Award of the SAE, and is currently a principal researcher within the Center of Excellence on Autonomous Marine Operations and Systems (AMOS).

Professor Roger Skjetne received in 2000 his MSc degree in control engineering at UCSB and his PhD degree in 2005 at NTNU, for which he was awarded the Exxon Mobil prize for best PhD thesis in applied research. Prior to his studies, he worked as an electrician for Aker Elektro AS on numerous oil installations for the North Sea. In 2004-2009, he was employed in Marine Cybernetics AS which offered services for independent verification by HIL simulation on safety-critical marine control systems. From August 2009 he has held the position of Professor in Marine Control Engineering at the Dept. of Marine Technology at NTNU. His research interests are within Arctic Dynamic Positioning and Ice Management systems for ships and rigs, environmentally robust control of electric power systems on ships and rigs, and nonlinear control theory for motion control of single and groups of marine vessels. Roger Skjetne is project manager for the Arctic DP research project, and associated researcher in the CoE Centre for Ships and Ocean Structures (CeSOS), CRI Sustainable Arctic Marine and Coastal Technology (SAMCoT), and CoE Autonomous Marine Operations and Systems (AMOS).

Eirik Mathiesen Eirik Mathiesen is a principal engineer at Kongsberg Maritime, responsible for application development of power management and dynamic positioning integration. He graduated from Vestfold University College and entered the Royal Norwegian Navy as an electrical supervisor in 1996. He joined Kongsberg Maritime in 1997 as a project engineer and has been involved with power management design for drillships and semi-submersible vessels on more than 50 instalations. Mathiesen is a co-holder of two patents on dynamic load prediction and dynamic load compensation.